Defect Detection in Plate Structures using Wavelet Transformation

Anna KNITTER-PIĄTKOWSKA, Michał GUMINIAK

Institute of Structural Engineering
Poznań University of Technology

Piotrowo 5, 60-965 Poznań, Poland
e-mail: {anna.knitter-piatkowska, michal.guminiak}@put.poznan.pl

This paper is concerned with defect detection in plate structures while considering the influence of external loads. The examined structures are based on Kirchhoff plate structures. Rectangular plate structures are considered. Plate bending is described using the boundary element method. The boundary and boundary-domain integral equations are formulated in a modified, simplified approach without the need of using a value known from the classical theory of Kirchhoff plate bending. Constant-type boundary elements in a non-singular approach are introduced. The plates are loaded with a single static concentrated force or dynamic moving force. External loading is applied at selected points along the direction parallel to one dimension of the plate. Defects are introduced by additional edges forming slots or holes in relation to the basic plate domain. Deflections and curvatures are taken into account as structural responses. Analysis of structural responses is conducted using the signal processing tool of wavelet transformation in its discrete form.

Key words: Kirchhoff plates, boundary elements, defect detection, wavelet transformation.

1. Introduction

The detection of defects is important for monitoring of a structural behaviour of engineering structures. There are several different non-destructive techniques, extensively investigated by scientists, which make it possible to identify the defective part of a structure. The approaches are based on, e.g., optimization of loads [1], information on natural frequencies [2], heat transfer [3], inverse analysis [4, 5], soft computing methods such as evolutionary algorithms [6] or artificial neural networks (ANNs) [7, 8]. Defects (damages) can be effectively detected using a relatively new method of signal analysis called wavelet transformation (WT) [9], as well as its discrete form (discrete wavelet transformation – DWT) [10–12]. By combining this method with ANN or inverse analysis, one can precisely identify defect (damage) details. This paper presents the case of

defect detection in thin plates excited by external static and dynamic loads. The influence of structural response signals on obtained results is considered too. Numerical examples are presented.

2. Theoretical considerations on wavelet transformation

Any considered signal can be expressed as a sum of sinusoidal signals. In this paper a wavelet transform will be implemented, in which for the representation of the signal $f(t)$, a linear combination of wavelet functions is used. In contrast to Fourier transform, wavelets are localized in the time and frequency domain. Therefore, they are well-suited for dealing with signals with discontinuities. The theory of WT was presented in many papers, e.g., in [13]. Below, the foundations of WT are presented and explained.

The continuous WT of the signal $f(t)$ in the time and frequency domain is defined as

$$(2.1) \qquad Wf(a,b) = \int_{-\infty}^{\infty} f(t) \cdot \overline{\psi}_{a,b}(t) \cdot dt,$$

where the overbar denotes the complex conjugate of the function under it. The function $\psi(t)$ is called the mother wavelet function and belongs to the field of $L^2(\mathbf{R})$. In addition to this, the function $\psi(t)$ must satisfy the condition of admissibility [13], which leads to equality

$$(2.2) \qquad \int_{0}^{\infty} \frac{|\Psi(\omega)|^2}{\omega} \cdot d\omega < \infty,$$

where $\Psi(\omega)$ is the Fourier transform of $\psi(t)$ and is defined as

$$(2.3) \qquad \Psi(\omega) = \int_{-\infty}^{\infty} \psi(t) \cdot e^{-i\omega t} \cdot dt.$$

The function $\Psi(\omega)$ is oscillatory because its average value is equal to zero:

$$(2.4) \qquad \int_{-\infty}^{\infty} \psi(t) \cdot dt = 0.$$

The mother wavelet function may have a real or complex-valued character. However, in the considered cases, real-valued wavelets are applied. For signal

decomposition, a set of wavelets (the wavelet family) are used and obtained by scaling and translating function ψ:

$$(2.5) \qquad \psi_{a,b} = \frac{1}{\sqrt{|a|}} \cdot \psi\left(\frac{t-b}{a}\right),$$

where t denotes the time or space coordinate, a is the scale parameter and b is the translation parameter. The parameters a and b take real values $(a, b \in (\mathbf{R}))$ and additionally $a \neq 0$. The element $|a|^{1/2}$ is the scale factor that ensures constant wavelet energy regardless of the scale. It means that $\|\psi_{a,b}\| = \|\psi\| = 1$ [14]. In the present numerical solution of the considered plate , the leading role is taken by DWT. In application, DWT requires neither integration nor explicit knowledge of scaling and wavelet functions. The wavelet family can be obtained by substituting $a = 1/2^j$ and $b = k/2^j$ into Eq. (2.5), which leads to the following relationship:

$$(2.6) \qquad \psi_{j,k}(t) = 2^{(j/2)} \cdot \psi(2^j \cdot t - k),$$

in which k and j are scale and translation parameters respectively. Meaning of these parameters for the simplest Haar wavelet is shown in Fig. 1.
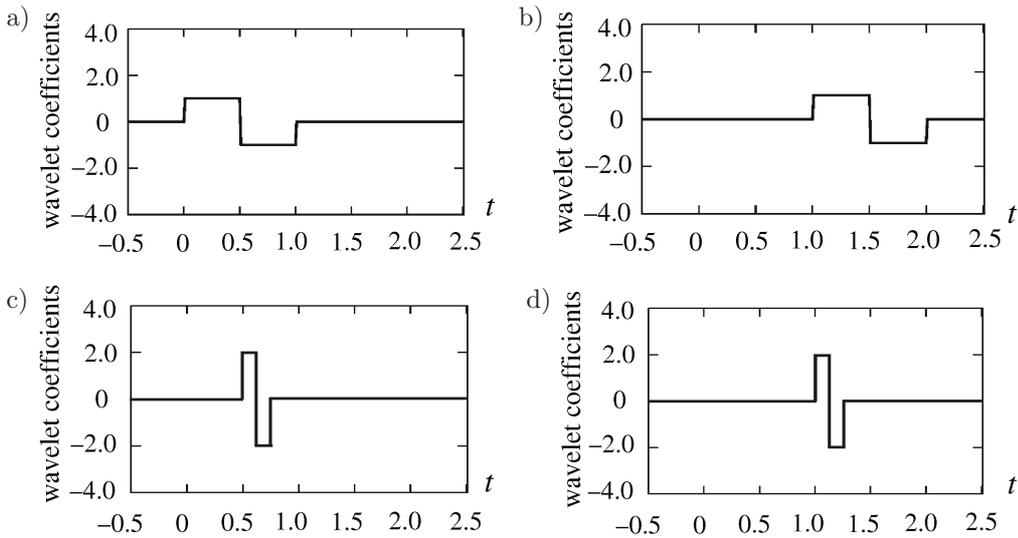

FIG. 1. Haar wavelet family: a) mother wavelet $j = 0$, $k = 0$, b) wavelet with parameters $j = 0$, $k = 1$, c) $j = 2$, $k = 2$, d) $j = 2$, $k = 4$.

Discrete signal decomposition can be written in the following form, according to the Mallat pyramid algorithm:

$$(2.7) \qquad f_J = S_J + D_J + ... + D_n + ... + D_1, \qquad n = J - j,$$

where each component in the signal representation is associated with a specific frequency range and provides information at the scale level ($j = 1, ..., J$). The discrete parameter J is the level of multi-resolution analysis (MRA) [13], S_J is a smooth signal representation, D_n and S_n are details and rough parts of a signal and D_1 corresponds with the most detailed representation of the signal. To fulfil the dyadic requirements of DWT, the function f_J must be approximated by $N = 2^J$ discrete values. The multi-resolution analysis according to the Mallat pyramid algorithm is illustrated in Fig. 2.
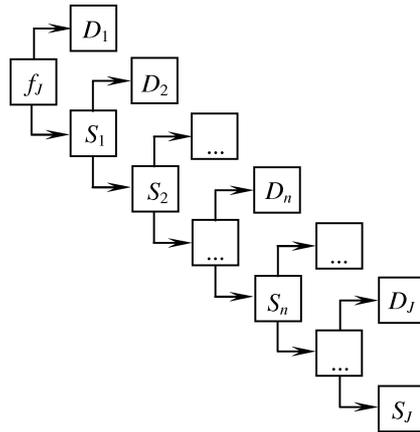
FIG. 2. Mallat pyramid algorithm [13].

In the analysis of defect detection, Daubechies wavelets are applied. This family of wavelet is orthogonal, continuous and has compact support. Daubechies wavelets are asymmetrical with sharp edges. They do not require a large number of coefficients; hence, they are widely used to solve a broad range of problems, e.g., image analysis or defect detection. The order of the functions of this wavelet family is contained between 2 and 20. The Daubechies wavelet of the second order corresponds to the simplest Haar wavelet. The basis and scaling functions of the Daubechies 4 wavelet are presented in Fig. 3.
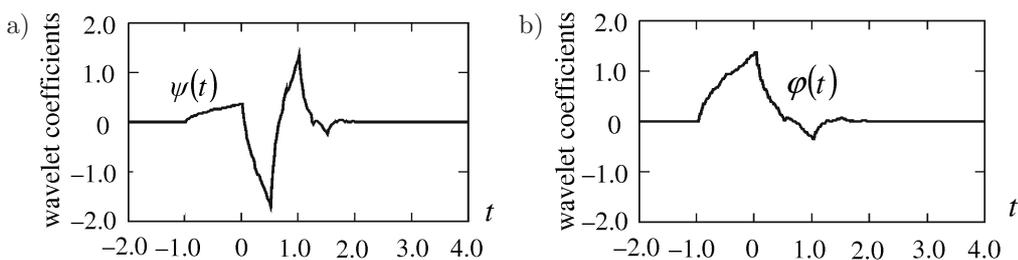
FIG. 3. (a) Basis function (mother) and (b) scaling function (father): Daubechies 4 wavelet.

3. DEFECT DETECTION – PROBLEM FORMULATION

The aim of this work is to detect the localization of defects providing that the defect (damage) exists in the considered plate structure. Numerical investigation is conducted based on signal analysis of structural static and dynamic responses. The plate material is assumed to be linear-elastic. The plate bending is described and solved by the boundary element method. The boundary integral equations are derived in a non-singular approach. Rectangular plates simply supported on the edges are considered. The analysis of structural responses is conducted with the use of a signal processing tool – DWT. Defects in plates are modelled as slots near the plate boundary. An example of a plate with a defected edge is illustrated in Fig. 4. A plate is loaded by a single concentrated force P moving along the indicated line, for example, 1), 2) or 3). The force P can have a static or dynamic character. At the selected point D, deflection w, angle of rotation in arbitrary direction ϕ, curvatures κ, internal forces, bending and twisting moments or transverse forces are measured as structural responses.
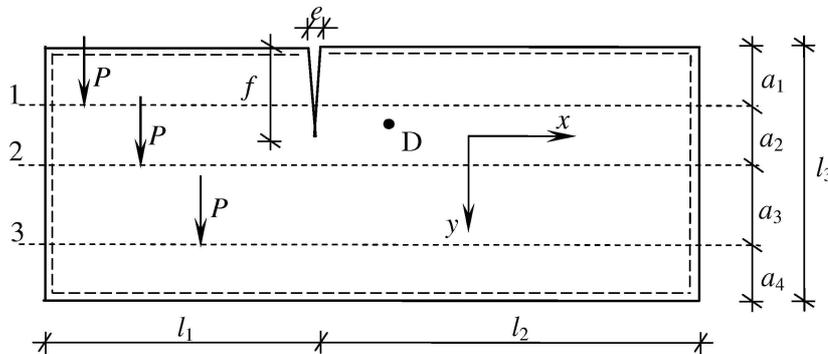

FIG. 4. Considered plate structure.

The measured response parameters have the character of influence lines in their discrete form. The signal of the structural response defined in this way is processed using DWT, which was described in Sec. 2.

The plate bending is described using the boundary element method in a simplified, modified approach where there is no need to introduce concentrated forces at the plate corners and equivalent shear forces at the plate continuous edges. This approach is used for static, dynamic and stability analysis in [15–18].

The boundary integral equations are derived using Betti's theorem. For static analysis of a plate subjected to the external distributed load q and the concentrated force P, the governing equations have the following form:

$$(3.1) \quad c(\mathbf{x}) \cdot w(\mathbf{x}) + \int\limits_{\Gamma} \left[T_n^*(\mathbf{y}, \mathbf{x}) \cdot w(\mathbf{y}) - M_{ns}^*(\mathbf{y}, \mathbf{x}) \cdot \frac{dw(\mathbf{y})}{ds} - M_n^*(\mathbf{y}, \mathbf{x}) \cdot \varphi_n(\mathbf{y}) \right]$$

$$\cdot \, d\Gamma(\mathbf{y}) = \int\limits_{\Gamma} \left[\widetilde{T}_n(\mathbf{y}) \cdot w^*(\mathbf{y}, \mathbf{x}) - M_n(\mathbf{y}) \cdot \varphi_n^*(\mathbf{y}, \mathbf{x}) \right] \cdot d\Gamma(\mathbf{y})$$

$$+ \int\limits_{\Omega} q(\mathbf{y}) \cdot w^*(\mathbf{y}, \mathbf{x}) \cdot d\Omega(\mathbf{y}) + P(i) \cdot w^*(i, \mathbf{x}),$$

$$(3.2) \quad c(\mathbf{x}) \cdot \varphi_n(\mathbf{x}) + \int\limits_{\Gamma} \left[\overline{T}_n^*(\mathbf{y}, \mathbf{x}) \cdot w(\mathbf{y}) - \overline{M}_{ns}^*(\mathbf{y}, \mathbf{x}) \cdot \frac{dw(\mathbf{y})}{ds} - \overline{M}_n^*(\mathbf{y}, \mathbf{x}) \cdot \varphi_n(\mathbf{y}) \right]$$

$$\cdot \, d\Gamma(\mathbf{y}) = \int\limits_{\Gamma} \left[\widetilde{T}_n(\mathbf{y}) \cdot \overline{w}^*(\mathbf{y}, \mathbf{x}) - M_n(\mathbf{y}) \cdot \overline{\varphi}_n^*(\mathbf{y}, \mathbf{x}) \right] \cdot d\Gamma(\mathbf{y})$$

$$+ \int\limits_{\Omega} q(\mathbf{y}) \cdot \overline{w}^*(\mathbf{y}, \mathbf{x}) \cdot d\Omega(\mathbf{y}) + P(i) \cdot \overline{w}^*(i, \mathbf{x}),$$

where the fundamental solution of the biharmonic equation

$$(3.3) \qquad\qquad \nabla^4 w^*(\mathbf{y}, \mathbf{x}) = \frac{1}{D} \cdot \delta(\mathbf{y}, \mathbf{x})$$

is given as Green's function

$$(3.4) \qquad\qquad w^*(\mathbf{y}, \mathbf{x}) = \frac{1}{8\pi D} \cdot r^2 \cdot \ln(r)$$

for a thin isotropic plate, $r = |\mathbf{y} - \mathbf{x}|$, δ is the Dirac delta, $\mathbf{x}$ is the source point, $\mathbf{y}$ is a field point, $D = \frac{Eh^3}{12 \cdot (1 - v^2)}$ is the plate stiffness, h is the plate thickness, and E and v are the Young modulus and the Poisson ratio respectively. The coefficient $c(\mathbf{x})$ is taken as

$c(\mathbf{x}) = 1$ when $\mathbf{x}$ is located inside the plate domain,

$c(\mathbf{x}) = 0.5$ when $\mathbf{x}$ is located on the smooth boundary,

$c(\mathbf{x}) = 0$ when $\mathbf{x}$ is located outside the plate domain.

The second boundary integral Eq. (3.2) can be obtained by replacing the unit concentrated force $P^* = 1$ with the unit concentrated moment $M_n^* = 1$. Such a replacement is equivalent to the differentiation of the first boundary integral Eq. (3.1) with respect to the co-ordinate n at point $\mathbf{x}$ belonging to the

plate domain. The expression $\widetilde{T}_n(\mathbf{y})$ denotes the shear force for clamped and for simply-supported edges [15–18]:

$$(3.5) \qquad \widetilde{T}_n(\mathbf{y}) = \begin{cases} V_n(\mathbf{y}), \\ R_n(\mathbf{y}). \end{cases}$$

Because the concentrated force at the corner is used only to satisfy the differential biharmonic equation of the thin plate, one can assume that this force could be distributed along a plate edge segment close to the corner [15–18]. The relation between $\varphi_s(\mathbf{y})$ and the deflection is known: $\varphi_s(\mathbf{y}) = \frac{dw(\mathbf{y})}{ds}$; the angle of rotation $\varphi_s(\mathbf{y})$ can be evaluated using a finite difference scheme of the deflection with two or more adjacent nodal values. In this analysis, the employed finite difference scheme includes the deflections of two adjacent nodes [18].

The forced vibration problem of a thin plate is considered too and the modal analysis is applied. Hence, the free vibration problem must be first solved. Inside a plate domain, additional collocation points associated with lumped masses are introduced according to Bezine technique [19]. In each internal collocation point, the vectors of displacement $w_i(t)$, acceleration $\ddot{w}_i(t)$ and inertial force $B_i(t)$ dependent on time t are established

$$w_i(t) = W_i \cdot \sin \omega t,$$

$$(3.6) \qquad \ddot{w}_i(t) = -\omega^2 \cdot W_i \cdot \sin \omega t,$$

$$B_i(t) = B_i \cdot \sin \omega t.$$

The inertial force amplitude is described as

$$(3.7) \qquad B_i = \omega^2 \cdot m_i \cdot W_i.$$

The boundary-domain integral equations have the character of amplitude equations and they are in the following form:

$$(3.8) \quad c(\mathbf{x}) \cdot w(\mathbf{x}) + \int_\Gamma \left[T_n^*(\mathbf{y}, \mathbf{x}) \cdot w(\mathbf{y}) - M_{ns}^*(\mathbf{y}, \mathbf{x}) \cdot \frac{dw(\mathbf{y})}{ds} - M_n^*(\mathbf{y}, \mathbf{x}) \cdot \varphi_n(\mathbf{y}) \right]$$

$$\cdot d\Gamma(\mathbf{y}) = \int_\Gamma \left[\widetilde{T}_n(\mathbf{y}) \cdot w^*(\mathbf{y}, \mathbf{x}) - M_n(\mathbf{y}) \cdot \varphi_n^*(\mathbf{y}, \mathbf{x}) \right] \cdot d\Gamma(\mathbf{y}) + \sum_{i=1}^{I} B_i \cdot w^*(\mathbf{i}, \mathbf{x}),$$

$$(3.9) \quad c(\mathbf{x}) \cdot \varphi_n(\mathbf{x}) + \int\limits_{\Gamma} \left[\overline{T}_n^*(\mathbf{y}, \mathbf{x}) \cdot w(\mathbf{y}) - \overline{M}_{ns}^*(\mathbf{y}, \mathbf{x}) \cdot \frac{dw(\mathbf{y})}{ds} - \overline{M}_n^*(\mathbf{y}, \mathbf{x}) \cdot \varphi_n(\mathbf{y}) \right]$$

$$\cdot d\Gamma(\mathbf{y}) = \int\limits_{\Gamma} \left[\widetilde{T}_n(\mathbf{y}) \cdot \overline{w}^*(\mathbf{y}, \mathbf{x}) - M_n(\mathbf{y}) \cdot \overline{\varphi}_n^*(\mathbf{y}, \mathbf{x}) \right] \cdot d\Gamma(\mathbf{y}) + \sum_{i=1}^{I} B_i \cdot \overline{w}^*(i, \mathbf{x}).$$

The set of algebraic equations in matrix notation has the following form:

$$(3.10) \quad \begin{bmatrix} \mathbf{G_{BB}} & \mathbf{G_{BS}} & -\lambda \cdot \mathbf{G_{Bw}} \cdot \mathbf{M_p} \\ \boldsymbol{\Delta} & -\mathbf{I} & \mathbf{0} \\ \mathbf{G_{wB}} & \mathbf{G_{wS}} & -\lambda \cdot \mathbf{G_{ww}} \cdot \mathbf{M_p} + \mathbf{I} \end{bmatrix} \cdot \begin{Bmatrix} \mathbf{B} \\ \varphi_\mathbf{S} \\ \mathbf{W} \end{Bmatrix} = \begin{Bmatrix} \mathbf{0} \\ \mathbf{0} \\ \mathbf{0} \end{Bmatrix},$$

where

$\mathbf{G_{BB}}$ and $\mathbf{G_{BS}}$ are the matrices of the dimensions $(2N \times 2N)$ and $(2N \times S)$, respectively, grouping boundary integrals and depending on the type of boundary, where N is the number of boundary nodes (or the number of constant-type elements) and S is the number of boundary elements along the free edge;

$\mathbf{G_{Bw}}$ is the matrix of the dimension $(2N \times M)$ grouping values of fundamental function w^* established at internal collocation points;

$\boldsymbol{\Delta}$ is the matrix grouping difference operators connecting angle of rotations in tangent direction with deflections of suitable boundary nodes if a plate has a free edge;

$\mathbf{G_{wB}}$ is the matrix of the dimension $(M \times 2N)$ grouping the boundary integrals of the appropriate fundamental functions, where M is the number of internal collocation points and N is the number of boundary nodes;

$\mathbf{G_{wS}}$ is the matrix of the dimension $(M \times S)$ grouping the boundary integrals of the appropriate fundamental functions;

$\mathbf{G_{ww}}$ is the matrix of the dimension $(M \times M)$ grouping the values of fundamental function w^* established at internal collocation points;

$\mathbf{M_p} = diag(m_1, m_2, m_3, ..., m_M)$ is the plate mass matrix, $\lambda = \omega^2$ and $\mathbf{I}$ is the unit matrix (M is the number of lumped masses). Elimination of boundary variables B and $\varphi_\mathbf{S}$ from matrix Eq. (3.10) leads to a standard eigenvalue problem:

$$(3.11) \qquad \left\{ \mathbf{A} - \widetilde{\lambda} \cdot \mathbf{I} \right\} \cdot \mathbf{W} = \mathbf{0},$$

where

$$\mathbf{A} = \left\{ \mathbf{G_{ww}} \cdot \mathbf{M_p} - (\mathbf{G_{wB}} - \mathbf{G_{wS}} \cdot \boldsymbol{\Delta}) \cdot [\mathbf{G_{BB}} + \mathbf{G_{BS}}]^{-1} \cdot \mathbf{G_{Bw}} \cdot \mathbf{M_p} \right\}.$$

4. Numerical examples

A rectangular plate structure simply-supported on its edges is considered. The boundary element method is applied to solve the thin plate bending problem. Each plate edge is divided into 30 constant-type boundary elements. The collocation point is located slightly outside the plate edge which is estimated by parameter $\varepsilon = \delta/d$, where δ is the real distance of the collocation point from the plate edge and d is the element length [15–17]. For each example $\varepsilon = 0.001$ is assumed. The diagonal boundary terms in the characteristic matrix are calculated analytically and other than diagonal terms are calculated using a 12-point Gauss quadrature. The plates properties are: $E = 205.0$ GPa, $v = 0.3$, $\rho = 7850$ kg/m^3, $h = 0.02$ m.

The plates are loaded statically and dynamically. The static concentrated external load $P = 1000$ N is replaced by the equivalent constant distributed loading q acting over the square surface of dimensions 0.05 m × 0.05 m. The dynamic concentrated force is harmonic: $P(t) = P_0 \cdot \sin pt$, where the amplitude is $P_0 = 1000.0$ N and $p = 10.0$ rad/s is the frequency of excitation. The damping coefficient is assumed to be $\mu = 0.1$. The first 100 natural frequencies and modes of the system are assumed using modal analysis. The plate mass matrix has the elements of the constant values. The number of internal collocation points associated with the lumped masses is equal to 200. It is also assumed that the harmonic excitation force moves slowly. Plate defects are introduced by the additional boundaries (free edges) forming a hole in relation to the basic plate domain [12]. A static and dynamic concentrated load is applied at selected points along the direction parallel to one dimension of the plate. As a structural response deflections and curvatures are taken into account as a structural response. The data are gathered in one measurement point, at equal time intervals. Decomposition of the obtained signal is carried out using DWT, Daubechies 4 wavelet functions.

4.1. Example 1

The plate loaded with a static concentrated force P is considered and presented in Fig. 5. The coordinates of the measurement point D are: $x_D = 2.15$ m and $y_D = 0.25$ m. The introduced plate defect is described by parameter $e = 0.005$ m.

It is clearly visible that in the case of the DWT (detail 1) of the vertical displacements (Fig. 6) and curvature κ_x (Fig. 7a) signals the damage was properly localized by the high peaks on these diagrams. In the case of the DWT of the curvature κ_y signal (Fig. 7b), the slot was also properly detected, but the area of disturbances was slightly wider.
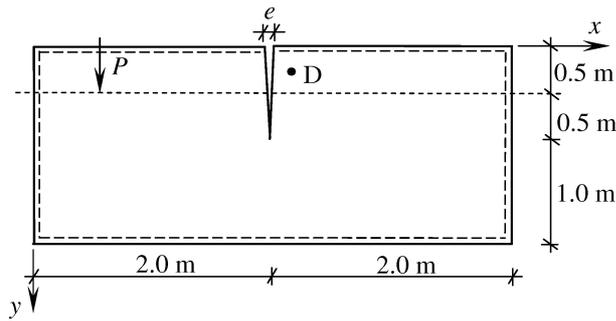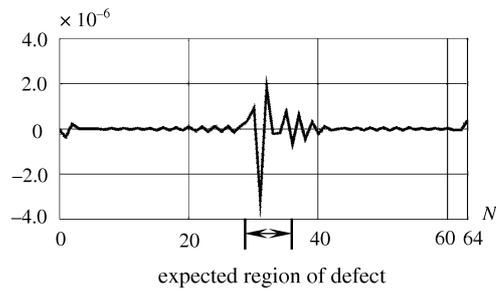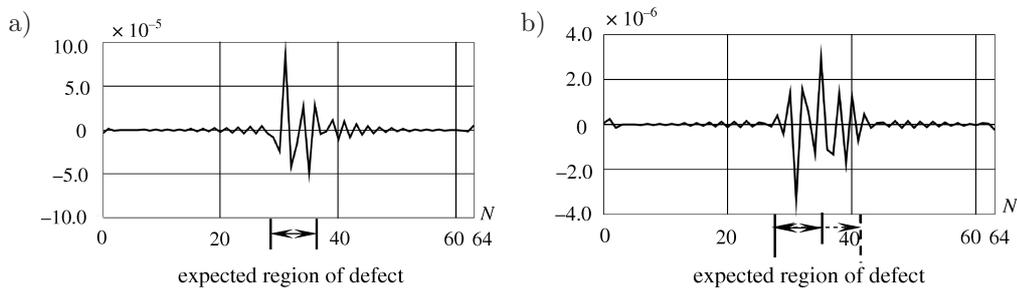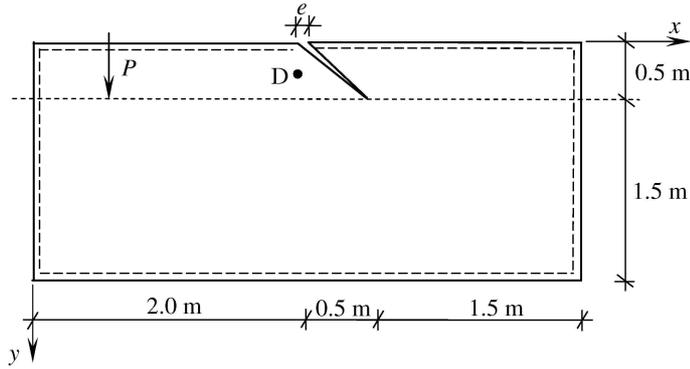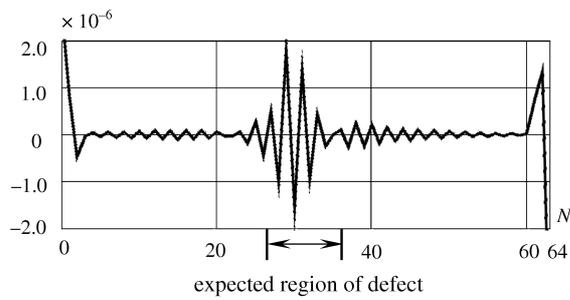
Fig. 5. Considered plate structure.

Fig. 6. DWT (Daubechies 4, detail 1) signal: vertical displacements measured at point D N – number of measurements.

Fig. 7. DWT (Daubechies 4, detail 1) signal: curvature κ_x (a) and κ_y (b) measured at point D, N – number of measurements.

4.2. Example 2

The plate loaded with a static concentrated force P is considered and presented in Fig. 8. The coordinates of the measurement point D are: $x_D = 2.0$ m and $y_D = 0.25$ m. The introduced plate defect is described by parameter $e = 0.005$ m.

FIG. 8. Considered plate structure.

Figures 9, 10a and 10b depict the DWT (detail 1) of the vertical displacements, curvature κ_x and curvature κ_y structural response signals respectively. In all three cases, the damage was properly detected by the evident disturbances of the transformed signal.

FIG. 9. DWT (Daubechies 4, detail 1) signal: vertical displacements measured at point D, N – number of measurements.
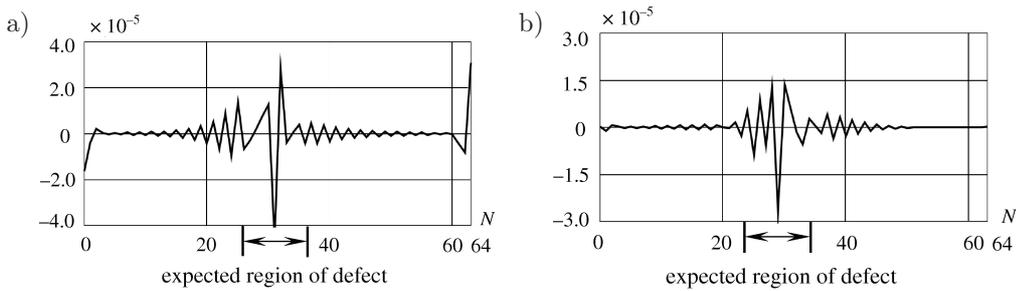

FIG. 10. DWT (Daubechies 4, detail 1) signal: curvature κ_x (a) and κ_y (b) measured at the point D, N – number of measurements.

4.3. Example 3

The plate loaded with a static concentrated force P is considered and presented in Fig. 11. The coordinates of the measurement point D are: $x_D = 2.35$ m and $y_D = 0.35$ m. The introduced plate defect is described by parameters $e_1 = e_2 = 0.005$ m.
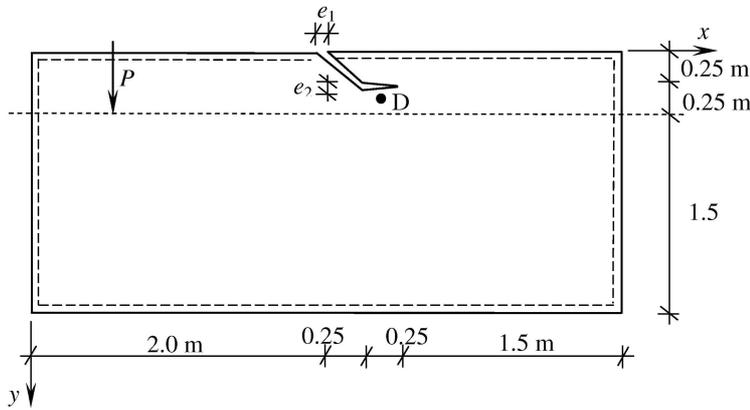

FIG. 11. Considered plate structure.

This example proves that it is possible to find quite accurately the beginning and end of the slot. It is visible that in the case of the DWT (detail 1) of the vertical displacements (Fig. 12) and curvature κ_x (Fig. 13a) signals, the disturbance area corresponds to the length of damage. However, in the case of the DWT of the curvature κ_y signal (Fig. 7b), the slot was properly detected, but the area of disturbances was slightly wider.
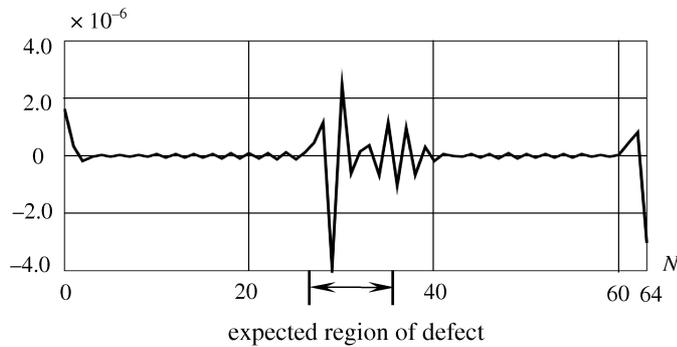

FIG. 12. DWT (Daubechies 4, detail 1) signal: vertical displacements measured at point D, N – number of measurements.
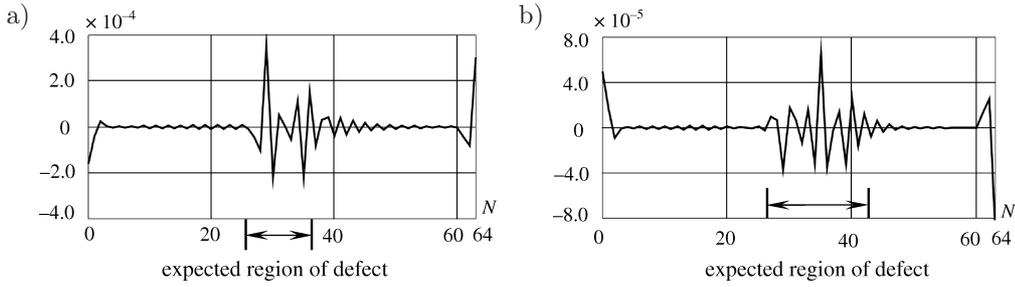
a)

b)

Fig. 13. DWT (Daubechies 4, detail 1) signal: curvature κ_x (a) and κ_y (b) measured at point D, N – number of measurements.

4.4. Example 4

The plate loaded with a static concentrated force P is considered and presented in Fig. 14. The coordinates of the measurement point D are: $x_D = 3.75$ m and $y_D = 0.35$ m. The introduced plate defect is described by parameters $e_1 = e_2 = e_3 = 0.005$ m.
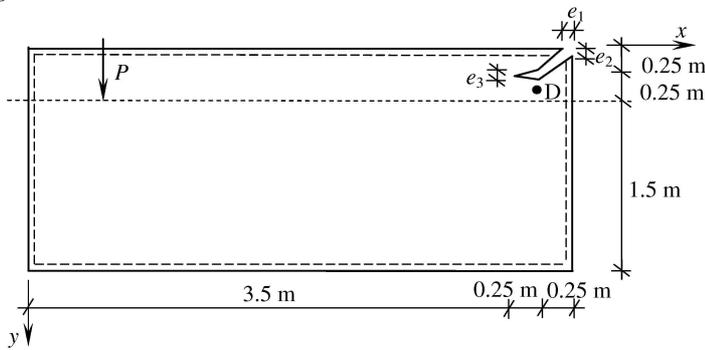

Fig. 14. Considered plate structure.

Detecting a failure in the corner of the plate is also possible. This is proven by the analysis results presented in Figs. 15, 16a and 16b. Evident disturbances
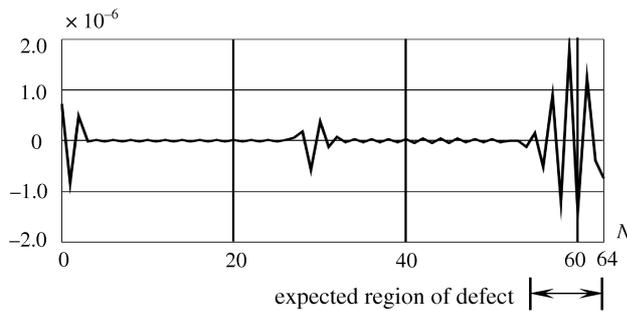

Fig. 15. DWT (Daubechies 4, detail 1) signal: vertical displacemens measured at point D, N – number of measurements.
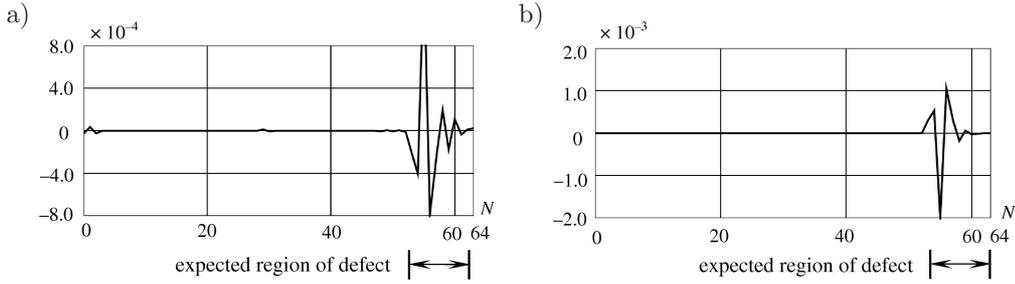
a)

b)

FIG. 16. DWT (Daubechies4, detail 1) signal: curvature κ_x (a) and κ_y (b) measured at point D,
N – number of measurements.

of the transformed vertical displacements (Fig. 15), curvature κ_x (Fig. 16a) and curvature κ_y (Fig. 16b) signals are indicators of the damage presence.

4.5. Example 5

The plate loaded with a static concentrated force P is considered and presented in Fig. 17. The coordinates of the measurement point D are: $x_D = 1.15$ m and $y_D = 1.75$ m. The introduced plate defect is described by parameters $e_1 = e_2 = e_3 = 0.005$ m.
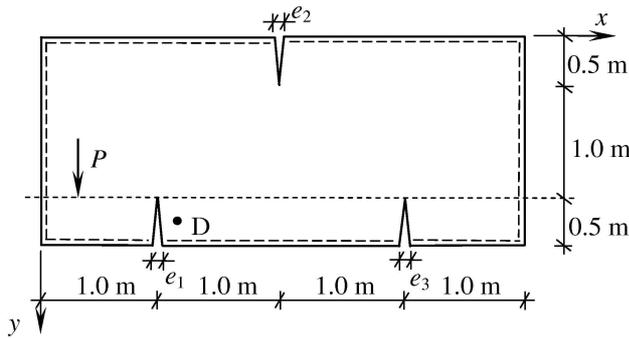
FIG. 17. Considered plate structure.

The authors also attempted to detect more than one failure in the plate structure. The effectiveness of approach strongly depended on the location of measurement point D. In this example, the best result was obtained when DWT was applied to analysis of the vertical displacement signal (Fig. 18), where two slots were properly detected. This was not so east to detect the two other transformations of the curvature κ_x (Fig. 19a) and curvature κ_y (Fig. 19b) signals, where only one defect was localized.
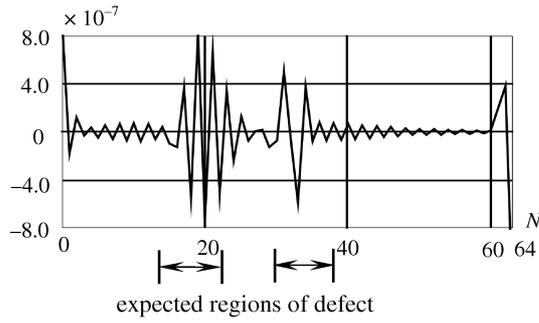
FIG. 18. DWT (Daubechies 4, detail 1) signal:
vertical displacements measured at point D, N –
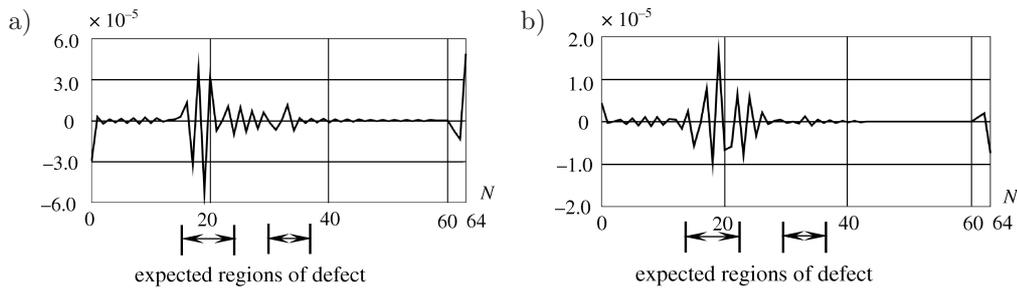number of measurements.

FIG. 19. DWT (Daubechies 4, detail 1) signal: curvature κ_x (a) and κ_y (b) measured at
point D, N – number of measurements.

4.6. Example 6

The plate loaded with a dynamic concentrated force $P(t) = P_0 \cdot \sin pt$ is considered and presented in Fig. 20. The coordinates of the measurement point D are: $x_D = 2.05$ m and $y_D = 0.3$ m. The introduced plate defect is described by parameter $e = 0.005$ m.
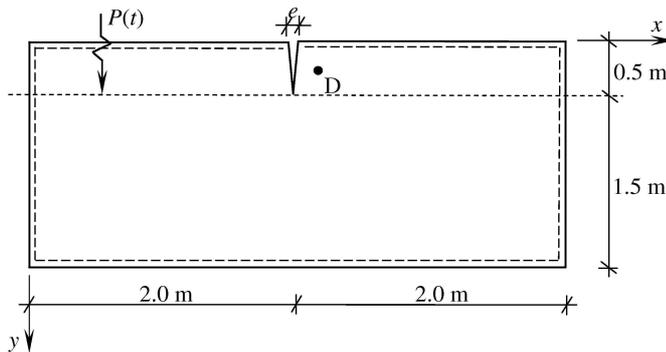

FIG. 20. Considered plate structure.

The defect in this example was also properly localized. A significant difference, in comparison to the experiments with static force excitation of the structure, is that the damage location is indicated here by the disturbances spread over a certain distance (Fig. 21). In previous examples, one high peak can be observed, e.g., in Fig. 6.
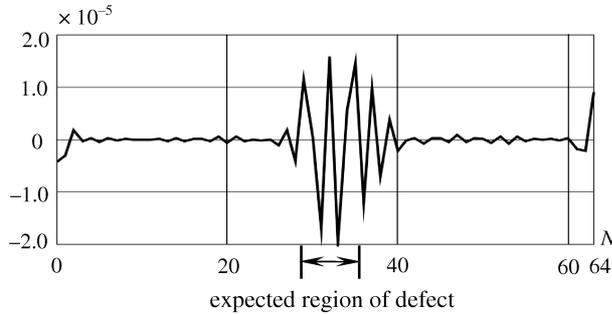

FIG. 21. DWT (Daubechies 4, detail 1) signal: amplitudes of the vertical displacements measured at point D, N – number of measurements.

5. CONCLUDING REMARKS

The implementation of discrete dyadic wavelet transformation to identify signal discontinuity in the analysis of plates is presented in this paper. The thin plate bending is described by boundary (static analysis) and boundary-domain (dynamic analysis) integral equations and solved using the boundary element method. Although the considered issue is two-dimensional from the point of view of deformation description, the application of one-dimensional DWT leads to satisfying results in defect detection. The analysis was carried out without any signal noise reduction. It was discovered that small disturbances in the response signal of a defective structure could be detected and the reference to a signal from an undamaged structure was not required (thereby avoiding additional errors). The novelty is that in this approach the data are gathered in one measurement point at equal time intervals. The distance of the measurement point from the damaged area is crucial for proper defect localization. The considered examples prove that DWT of structural response signal expressed in deflections or curvatures established at selected domain points quite correctly identifies the presence and position of a defect. The effectiveness of the proposed method is indicated by the presented numerical investigation, where the defects are properly localized, even for the relatively small number of measurements.

References

1. Mróz Z., Garstecki A., *Optimal loading conditions in design and identification of structures. Part 1: Discrete formulation*, International Journal of Structural and Multidisciplinary Optimization, **29**(1): 11–18, 2005.

2. Dems K., Mróz Z., *Identification of damage in beam and plate structures using parameter dependent frequency changes*, Engineering Computation, **18**(1/2): 96–120, 2001.

3. Ziopaja K., Pozorski Z., Garstecki A., *Damage detection using thermal experiments and wavelet transformation*, Inverse Problems in Science and Engineering, **19**(1): 127–153, 2011.

4. Garbowski T., Maier G., Novati G., *Diagnosis of concrete dams by flat-jack tests and inverse analysis based on proper orthogonal decomposition*, Journal of Mechanics of Materials and Structures, **6**(1–4): 181–202, 2011.

5. Knitter-Piątkowska A., Garbowski T., *Damage detection through wavelet decomposition and soft computing*, International Conference on Adaptive Modelling and Simulation ADMOS 2013, Lisbon, Portugal, June 3–5, 2013, peer-review article in proceeding, J.P. Moitinho de Almeida, P. Díez, C. Tiago, N. Parés [Eds.], CIMNE Barcelona, pp. 389–400, 2013.

6. Burczyński T., Kuś W., Długosz A., Orantek P., *Optimization and defect identification using distributed evolutionary algorithms*, Engineering Applications of Artificial Intelligence, **17**(4): 337–344, 2004.

7. Rucka M., Wilde K., *Neuro-wavelet damage detection technique in beam, plate and shell structures with experimental validation*, Journal of Theoretical and Applied Mechanics, **48**(3): 579–604, 2010.

8. Waszczyszyn Z., Ziemiański L., *Neural networks in mechanics of structures and materials – new results and prospects of application*, Computers and Structures, **79**(22–25): 2261–2276, 2001.

9. Wang Q., Deng X., *Damage detection with spatial wavelets*, International Journal of Solids and Structures, **36**(23): 3443–3468, 1999.

10. Knitter-Piątkowska A., Pozorski Z., Garstecki A., *Application of discrete wavelet transformation in damage detection. Part I: Static and dynamic experiments*, Computer Assisted Mechanics and Engineering Sciences, **13**(1): 21–38, 2006.

11. Knitter-Piątkowska A., Guminiak M., Przychodzki M., *Damage detection in truss structure being the part of historic railway viaduct using wavelet transformation*, [in:] Recent Advances in Computational Mechanics, CRC Press/Balkema, Taylor and Francis Group, T. Łodygowski, J. Rakowski, P. Litewka [Eds.], pp. 157–163, 2014.

12. Knitter-Piątkowska A., Guminiak M., *Damage detection in plate structures using wavelet transformation*, Proceedings of 39th Solid Mechanics Conference, SOLMECH–2014, Book of Abstracts, pp. 157–158, September 1–5, Zakopane, Poland, 2014.

13. Mallat S.G., *A theory for multiresolution signal decomposition: The wavelet representation*, IEEE Transactions on Pattern Analysis and Machine Intelligence, **11**(7): 674–693, 1998.

14. Strang G., Nguyen T., *Wavelets and filter banks*, Wellesley-Cambridge Press, Wellesley, 1996.

15. Guminiak M., *Static analysis of thin plates by the Boundary Element Method in a non-singular approach*, Foundations of Civil and Environmental Engineering, **9**: 75–93, 2007.

16. Guminiak M., Sygulski R., *Vibrations of plates immersed in compressible fluid by the BEM*, Proceedings of 9th International Conference Modern Building Materials, Structures And Techniques, Vilnius, May 16–18, 2007, Selected Papers, Vilnius Gediminas Technical University Press "Technika" scientific book 1435, pp. 925–930, 2007, M.J. Skibniewski, P. Vainiunas and E.K. Zavadskas [Eds.].

17. Guminiak M., Sygulski R., *Vibrations of system of plates immersed in fluid by BEM*, Proceedings of III European Conference on Computational Mechanics, Solids, Structures and Coupled Problems in Engineering ECCM–2006, June 5–9, 2006, Lisbon, Portugal. Springer 2006, C.A. Mota Soares, J.A.C. Rodrigues, J.A.C. Ambrósio, C.A.B. Pina, C.M. Mota Soares, E.B.R. Pereira, J. Folgado [Eds.], p. 211, CD enclosed.

18. Guminiak M., *An alternative approach of initial stability analysis of Kirchhoff plates by the Boundary Element Method*, Engineering Transactions, **62**(1): 33–59, 2014.

19. Bèzine G., Gamby D.A., *A new integral equation formulation for plate bending problems*, [in:] Recent Advances in Boundary Element Method, C.A. Brebbia [Ed.], Pentech Press, London, 1978.